HHS Public Access

Author manuscript

Pharmacogenomics. Author manuscript; available in PMC 2018 July 11.

Published in final edited form as:

Pharmacogenomics. 2014 April ; 15(6): 759–774. doi:10.2217/pgs.14.39.

Developmental and extracellular matrix-remodeling processes in rosiglitazone-exposed neonatal rat cardiomyocytes

Paul Paolini[‡,1,2], **Daniel Pick**[3], **Jennifer Lapira**[4], **Giuseppina Sannino**[4,5], **Lorenza Pasqualini**[4,6], **Colleen Ludka**[4], **L James Sprague**[4], **Xian Zhang**[2], **Elesha A Bartolotta**[1], **Esteban Vazquez-Hidalgo**[2], **David Torres Barba**[2], **Carlos Bazan**[2], and **Gary Hardiman**[*,‡,2,4,7,8]

[1]Department of Biology, San Diego State University, CA, USA

[2]Computational Science Research Center, San Diego State University, CA, USA

[3]Institute of Mathematical Sciences, Claremont Graduate University, Claremont, CA, USA

[4]University of California San Diego, School of Medicine, La Jolla, CA, USA

[6]LP, Innsbruck Medical University, Department of Urology, Innsbruck, Austria

[7]Biomedical Informatics Research Center, San Diego State University, CA, USA

[8]Department of Medicine, Medical University of South Carolina, Charleston, SC, USA

Abstract

Objective—The objective of this study was to investigate the effects of rosiglitazone (Avandia®) on gene expression in neonatal rat ventricular myocytes.

Materials & methods—Myocytes were exposed to rosiglitazone *ex vivo*. The two factors examined in the experiment were drug exposure (rosiglitazone and dimethyl sulfoxide vs dimethyl sulfoxide), and length of exposure to drug (1/2 h, 1 h, 2 h, 4 h, 6 h, 8 h, 12 h, 18 h, 24 h, 36 h and 48 h).

Results—Transcripts that were consistently expressed in response to the drug were identified. Cardiovascular system development, extracellular matrix and immune response are represented prominently among the significantly modified gene ontology terms.

[*]Author for correspondence: hardiman@musc.edu.

[5]Current address: GS, Natural & Medical Sciences Institute, University

[‡]Authors contributed equally

Financial & competing interests disclosure

The authors have no other relevant affiliations or financial involvement with any organization or entity with a financial interest in or financial conflict with the subject matter or materials discussed in the manuscript apart from those disclosed.

No writing assistance was utilized in the production of this manuscript.

Ethical conduct of research

The authors state that they have obtained appropriate institutional review board approval or have followed the principles outlined in the Declaration of Helsinki for all human or animal experimental investigations. In addition, for investigations involving human subjects, informed consent has been obtained from the participants involved.

Conclusion—*Hmgcs2, Angptl4, Cpt1a, Cyp1b1, Ech1* and *Nqo1* mRNAs were strongly upregulated in cells exposed to rosiglitazone. Enrichment of transcripts involved in cardiac muscle cell differentiation and the extracellular matrix provides a panel of biomarkers for further analysis in the context of adverse cardiac outcomes in humans.

Keywords

Avandia®; neonatal rat ventricular myocytes; NRVMs; peroxisome; PPAR-γ; proliferator-activated receptor-γ; rosiglitazone; T2DM; Type 2 diabetes mellitus

The prevalence of Type 2 diabetes mellitus (T2DM) is increasing rapidly in the US and afflicting more than 25.8 million children and adults, or roughly 8.3% of the population. Diabetes prevalence varies by race and ethnicity. African–Americans have the highest prevalence (12.6%), followed closely by Hispanics (11.8%), Asian–Americans (8.4%) and white subjects (7.1%) [1]. The total annual global health expenditure for diabetes in 2010 was estimated to reach minimally US$376.0 billion, with diabetes accounting for 12% of the world's total health expenses [2].

Rosiglitazone (Avandia®, 1999, GlaxoSmithKline, PA, USA), a member of the thiazolidinedione (TZD) family of insulin-sensitizing drugs, is widely used as a therapeutic to treat Type 2 diabetes. TZDs are selective agonists of the nuclear receptor PPAR-γ [3–5].

Many studies to date have explored the cardioprotective effects of TZDs on the heart. Rosiglitazone improves diastolic myocardial function in T2DM patients by reducing oxidative stress and inflammation suggesting that it provides significant cardiac benefit [6]. In animal models of diabetes, TZDs reduced ischemia-reperfusion myocardial injury by reducing both inflammation and insulin resistance [7]. Another prevalent T2DM cardiovascular condition for which TZDs have improved health status is in the treatment of hypertension, indicating that TZD therapy provides benefit for treatment of hypertension, thereby lowering the risk for potential vascular complications [8]. Additionally, TZDs may provide beneficial antiatherogenic effects including increasing high-density lipoprotein cholesterol levels and low-density lipoprotein particle size, and decreasing triglyceride levels. Positive effects have been obtained with TZDs improving the dyslipidemic profiles commonly observed in T2DM [9]. Rosiglitazone also increases levels of high-density lipoprotein 2 cholesterol, a class beneficial for the heart [10]. Furthermore in a canine model, rosiglitazone reduced harmful levels of intramyocyte lipid accumulation in the myocardia of dyslipidemic dogs [11].

Despite the cardioprotective effects mediated by rosiglitazone, cardiovascular disease is the leading cause of death among diabetic patients [8,12]. Controversy has surrounded the safety of rosiglitazone in recent years with conflicting reports indicating either increased risk or lack of statistically significant increase in myocardial infarction [8,13]. Concern about its adverse effects has reduced use of the drug despite its efficacy for glycemic control [14]. In the US, rosiglitazone remains on the market although it is subject to significant restrictions [15]. In Europe, the EMA recommended in September 2010 that the drug be suspended [16].

Although previous work has demonstrated a potential link between the effects of rosiglitazone and NF-κB-dependent pathways, the exact signaling pathways through which rosiglitazone regulates its effects on the heart remain largely unknown [17]. Rosiglitazone is a high affinity agonist for PPAR-γ [8,18–22] and PPAR-γ agonists have very diverse biological effects, resulting from the activation and suppression of many genes each involved in one or more molecular signaling pathways [8,23].

For many years neonatal rat ventricular myocytes (NRVMs) cultured *in vitro* have served as a model for recreating and studying several cardiac molecular conditions, including hypertrophy and oxygen deprivation. NRVMs are postmitotic terminally differentiated cells, which do not divide, yet express both cardiac myosin isoforms (α/β-*MyHC*), beat spontaneously and respond to different pharmacological stimuli [24,25].

There remains a need to better classify both the gene targets and molecular signaling pathways to fully comprehend the beneficial and potentially adverse effects of rosiglitazone. To further this objective, we undertook a series of genome-wide expression-profiling experiments using NRVMs. The ability to culture these cells for an extended period makes them an ideal system to study the longitudinal effects of rosiglitazone treatment on cardiac gene expression.

Materials & methods

Materials & neonatal rat ventricular myocytes

Neonatal rat ventricular myocytes were isolated from 1–4 day old Harlan Sprague-Dawley Rats (*Rattus norvegicus albinus*), and cultured as described previously [17]. Cultures prepared by this method contain >98% cardiac myocytes. All animal procedures were in accordance with the San Diego State University Animal Subjects Committee (UASC) and NIH Animal Welfare Assurance A3728-01. After preplating the myocytes to remove fibroblasts, pooled myocytes were centrifuged and resuspended in DMEM/F-12 (Gibco, Life Technologies, CA, USA) containing 10% fetal bovine serum (Irvine Scientific, CA, USA). Myocytes were subsequently plated on Fibronectin (Gibco)-coated 100 mm dishes overnight to allow for recovery and washed twice with 1:1 medium consisting of DMEM/F-12, kanamycin, ampicillin, and fungizone on the following day. Cells were then incubated overnight in a minimal medium, which was the same as the 1:1 medium, but supplemented with 1 mg/ml bovine serum albumin (Sigma, MO, USA). On the third day, cells were washed two more times with 1:1 medium and replaced with an Insulin-Transferrin-Selenium medium consisting of minimal medium, 1X Insulin-Transferrin-Selenium (Life Technologies), 0.4X MEM nonessential amino acids mixture (Sigma), and 0.1X MEM vitamins medium (Invitrogen, CA, USA) in the presence or absence of 10 μmol/l rosiglitazone or 1% dimethyl sulfoxide (DMSO). Rosiglitazone was obtained from GlaxoSmithKline, and stock solutions were prepared in 1% DMSO.

Study design

We used an 11 × 2 factorial design. The factors examined in the experiment were drug exposure (rosiglitazone + DMSO, and DMSO only), and length of exposure to drug (1/2 h, 1

h, 2 h, 4 h, 6 h, 8 h, 12 h, 18 h, 24 h, 36 h and 48 h). The objective of these experiments was to study the effects of rosiglitazone on NRVMs over time. To discriminate the effects of the drug from that of the vehicle (DMSO), a comparison of rosiglitazone plus DMSO versus DMSO only was performed. Specifically, NRVM cells were exposed to each of the possible combinations of the two factors (drug and time) outlined above. Two biological replicates were performed for each combination and this resulted in 44 samples for analysis. The 1% DMSO only control discriminated DMSO specific effects from rosiglitazone effects on cellular gene expression. The concentration of rosiglitazone (10 μmol/l) was selected based on previous work from this group examining the cardioprotective effects of rosiglitazone on NRVMs by measuring Ca^{2+} transient decay rates and *SERCA2* gene expression [17].

Isolation of total RNA for microarray studies

NRVM cells were placed directly in 1 ml TRIzol reagent prior to nucleic acid extraction. The TRIzol protocol was followed as recommended by the manufacturer (Invitrogen). Briefly, the total RNA was precipitated, purified and air-dried. The pellet was subsequently resuspended in a solution of water, DNase buffer and DNase enzyme (Qiagen, CA, USA), and incubated at room temperature for 10 min to remove any genomic DNA contamination. Total RNA was then purified on a Qiagen RNeasy® column according to manufacturer's instructions. Elution was carried out with RNase/DNase-free water in two parts, combined and concentrated using a Savant™ Integrated SpeedVac™ Vacuum System (Thermo Scientific Inc., MA, USA) until the total volume reached 15 μl. For RNA quantification, 1 μl of total RNA was used to measure the absorbance at 260 nm of each sample by means of the NanoDrop ND-1000 (NanoDrop Technologies, DE, USA). The samples were then transported to the UCSD BIO-GEM core for Illumina (CA, USA) Beadarray processing.

DNA microarray experiments

Biotinylated cRNA was prepared using the Illumina RNA Amplification kit, Catalog #1L1791 (Ambion, Inc., TX, USA) according to the manufacturer's directions, starting with 250 ng total RNA. For microarray analysis, the RatRef-12 Expression BeadChip was used (Illumina). Hybridization of labeled cRNA to the BeadChip, and washing and scanning were performed according to the Illumina BeadStation 500× manual. Essentially, the amplified, biotin-labeled human cRNA samples were resuspended in a solution of Hyb E1 buffer (Illumina) and 25% (v/v) formamide at a final concentration of 25 ng/μl. A total of 1.5 μg of each cRNA was hybridized. Hybridization was allowed to proceed at 55°C, for 18 h after which, BeadChip was washed for 10 min with 1X high temperature buffer (Illumina), followed by a subsequent 10 min wash in Wash E1BC buffer. The arrays were then washed with 100% ethanol for 10 min to strip off any remaining adhesive on the chip. A 2 min E1BC wash was performed to remove residual ethanol. The arrays were blocked for 5 min with 1% (w/v) casein–phosphate buffered saline (Pierce Biotechnology, IL, USA). The array signal was developed via 10 min incubation with streptavidin-Cy3 at a final concentration of 1 μg/ml solution of (GE Healthcare, Buckinghamshire, UK) in 1% casein–phosphate buffered saline blocking solution. The expression BeadChip was washed a final time in Wash E1BC buffer for 5 min and subsequently dried via centrifugation for 4 min at a setting of 275 rcf.

The arrays were scanned on the Illumina BeadArray reader, a confocal-type imaging system with 532 (cye3) nm laser illuminations. Image analysis and data extraction was carried out in accordance with Illumina specifications. Preliminary data analysis and quality control was carried out using the GenomeStudio software (Illumina). All array data has been deposited in the EBI ArrayExpress database. The ArrayExpress accession number is E-MTAB-2426.

Microarray data analysis

RatRef-12 BeadChip annotation—The RatRef-12 BeadChip contained 22,523 probes selected primarily from the NCBI RefSeq database. In order to improve the annotation of the array probes we aligned all the 50-mer probes with the complete *Rattus norvegicus* transcriptome, allowing at most three mismatches for the alignments.

Normalization of microarray data—Expression level data from the Illumina BeadStudio software were normalized using a multiple-Loess algorithm [26]. Probes whose expression level exceeds a threshold value in at least one sample were called detected. The threshold value was found by inspection from the distribution plots of ($\log_2$) expression levels.

Time course analysis & sorting of genes according to significance—Detected probes were sorted according to their q-value, which is the smallest false-discovery rate at which the gene is called significant [27]. We evaluated q-values of genes in the full 48-h two-class unpaired time course analysis using significance analysis of microarrays (SAM) algorithm and its implementation in the official statistical package *samr* for R [28–30]. In order to not be unduly impressed by accidentally small variances, we set the percentile of standard deviation values used for the exchangeability factor *s0* in the test statistic to 75.

Nonparametric analysis of gene expression in stages I, II & III—A *post hoc* inspection of the gene-expression time course inspired us to divide the time course into three stages: early (stage I, 0.5–2 h), intermediate (stage II, 4–18 h) and late (stage III, 24–48 h). Proceeding on a hypothesis that these groups may represent distinct stages of the drug's action, we attempted to gain statistical power by treating the separate time points within each group as replicates at the level of gene ranks. In this analysis, genes are ranked at each time point by the $\log_2$ ratio of expression (average $\log_2$ ratio is taken from the two true biological replicates at each point) in rosiglitazone vs DMSO. Even if the neighboring time points are not exactly equivalent, the ranking of genes may be sufficiently similar to indicate patterns. At each stage, ranks of each gene are added to form a rank-sum statistic (there are n = 3 ranks to be added in stage I, n = 5 in stage II, and n = 3 in stage III). A q-value is assigned to each gene based on the null model in which the rank-sum statistic is formed by adding n integers randomly from a uniform distribution, with replacement. The exact closed-form expression for the distribution of the rank-sum statistic for uniform variates is known and can be used with great accuracy for sums of discrete ranks when the number of genes is large [31].

Statistical analysis of pathways & gene ontology terms—Each gene ontology (GO) term or a pathway is treated simply as a set of genes. The probe list, sorted by q-value

in ascending order, is translated into Entrez gene IDs and parsed so that whenever several different probes represent the same gene, only the highest-ranking probe is kept for further analysis. The sorted list of genes is subjected to a nonparametric variant of the Gene Set Enrichment Analysis (GSEA) [32], in which the p-value of a gene set of size n is defined as follows: Let us denote the *k*-th highest rank in gene set as *rk*, and define *pk* as the probability that out of n randomly chosen ranks (without replacement) the *k*-th highest is not smaller than *rk*. The p-value of the gene set is defined as min*k* (*pk*). It is designed to detect over-represented gene sets at the top of the sorted gene list. Unlike the Kolmogorov–Smirnov statistic used in GSEA, it will not detect under-represented, or other pathologically distributed, gene sets. Finding the p-value of a gene set of size n requires calculation of n rank-order values *pk*; however, there is no need to adjust the p-values for multiple testing as the rank-order tests are highly statistically dependent. We do perform a Bonferroni adjustment of gene set p-values for the number of gene sets tested, even though there are often several gene sets with overlapping gene content (and therefore are statistically dependent). In part this is due to the hierarchical design of the GO database and partly because genes tend to be involved in multiple processes. We report only gene sets with adjusted p-values ≤0.01. Heat maps of expression levels were created using in-house hierarchical clustering software that implements Ward clustering. The colors qualitatively correspond to fold changes with respect to a reference that is calculated as the mid-point between compared groups.

Information clustering & principal coordinate analysis—A typical list of significant GO terms usually contains redundant, closely related terms with very little difference in member genes in addition to informative terms. In order to reduce redundancy of reporting, we cluster the significant terms using a distance metric called variation of information [33,34]. A mutual distance matrix so obtained is used to cluster the significant GO terms, which is visualized in two dimensions using a principal coordinates analysis (multiscaling) function *cmdscale* of R [29,30]. We use this visualization to report the relevant nonredundant set of significant GO terms at stages I, II and III.

Quantitative real-time PCR analysis—In order to investigate further the molecular effects of rosiglitazone, we employed quantitative PCR (Q-PCR). Q-PCR was performed to validate the differential microarray expression patterns of selected genes using the same group of NRVMs exposed to rosiglitazone and DMSO. Relative mRNA transcript levels were measured by real-time quantitative RT-PCR in a LightCycler 480® (Roche Applied Science, CA, USA). Total RNA reverse-transcribed using the Roche Transcriptor kit (Roche Applied Science) and 50 ng cDNA was quantified using the LightCycler 480 SYBR Green Master kit (Roche Applied Science, IN, USA). Duplicate biological samples were used. Each individual sample was run as a technical triplicate and geometric mean values were reported. The results were examined using a one-way ANOVA followed by a Tukey test, using the statistical software GraphPad Prism version 5.0 (GraphPad Prism Software, Inc., CA, USA). The *Gapdh* mRNA served as an internal control for normalization. Normalized gene expression values were obtained using LightCycler Relative Quantification software (Roche Applied Science). Relative gene copy numbers were derived by efficiency-corrected relative quantification using the formula $2^{\Delta CT}$ where ΔCT is the difference in amplification

cycles required to detect amplification product from equal starting concentrations of RNA. Results were expressed as fold change compared with untreated cells. Individual forward and reverse primers were used as described in the supplementary material (Supplementary Table 1; www.futuremedicine.com/doi/suppl/10.2217/pgs.14.39).

Results

Neonatal cardiomyocyte purity

Noncardiocyte contamination was estimated to be less than 1%. Cells were counted from three plates and 500 cells counted on each plate were neonatal cardiocytes. There were 1500 neonatal cardiocytes in total and a total of 13 fibroblasts across the three plates. This corresponds to a cell purity estimate of 99.1%.

RatRef-12 BeadChip annotation

In order to improve the annotation of the 22,523 probes on the Illumina RatRef-12 BeadChip, which were based on NCBI RefSeq database (Release 16) we employed the SeqMap alignment program to align all the 50-mer probes with the complete *Rattus norvegicus* transcriptome, allowing at most 3 bp mismatches for the alignments [35]. These facilitated mapping of the majority of the transcripts onto genes. In some cases, alignments with three mismatches represented the optimal hit obtained. However in the majority of cases, perfect alignments were achieved against the rat transcriptome. When more than three mismatches were obtained with the alignments, these probes were discarded and not included in the downstream data analysis. Many of the probes lacking annotation information in the original descriptor derived from cDNA libraries and expressed sequencing tag efforts. After this reannotation of the RatRef-12 BeadChip, 16,600 probes were present with Entrez gene ID fields. The updated annotation is provided in the supplementary material (Supplementary Table 2).

GO analysis of the rosiglitazone time course

After the data were normalized, genes were ranked according to interest based on their expression patterns across the entire 48 h time course, and statistical analysis of enriched GO terms was performed. The results of these analyses are presented in Table 1. The GO terms ‘lipid metabolic process’, ‘response to lipid’ and ‘immune response’ were significantly enriched (Table 1). The terms lipid metabolic process and immune response are presented in Figures 1 & 2, respectively as heat maps to view differential transcript expression. All transcripts in these figures were significant at false-discovery rate <0.05 in the entire time course comparison. The majority of the transcripts in the lipid metabolic process category were upregulated with the strongest induction occurring later in the time course. The majority of the immune response transcripts were downregulated towards the end of the rosiglitazone exposure time course.

GO & pathway analysis of the rosiglitazone time course segmented into early, intermediate & late stages

As we wished to better explore the temporal effects associated with exposure to the drug using NRVMs, we stratified the data set into three different stages, representing immediate,

intermediate and late gene-expression profiles as outlined above, and carried out GO analyses. Owing to the overlap of gene membership among GO terms, significant terms should not be reported as independent gene sets. We therefore clustered significant gene sets using variation of information as the distance metric [33,34], and present them graphically in this context using a principal coordinates analysis (Figure 3). Variation of information between two gene sets is also called shared information, and is a true metric. Significant biological process GO terms at stages I, II and III are outlined in Tables 2, 3 & 4, respectively. The GO term ‘cardiovascular system development’ was a significantly enriched biological process in stages I, II and III, respectively (Figure 3 & 4, & Tables 2, 3 & 4). The GO term ‘blood vessel morphogenesis’ was another biological process significantly enriched in stages I and III, respectively (Figure 3, & Tables 2 & 4). The GO cellular component term ‘extracellular matrix’ was significantly enriched in stage III (Figure 5 & Table 5).

Validation by Q-PCR

In order to validate these findings and further understand the changes that occur in NRVMs we employed Q-PCR. To verify the microarray results and better investigate the potential adverse effects of rosiglitazone on some of the key transcripts identified as significantly altered, we performed Q-PCR measurements of abundance of five transcripts: *Hmgcs2, Angptl4, Cpt1a, Cyp1b1* and *Ech1*. These represent transcripts that were identified as strongly upregulated in the exposed cells and play roles in key lipid metabolic processes. We chose transcripts relevant to lipid metabolism as this was the strongest response observed with the array data analysis.

Additionally *Angptl4* belongs to the GO biological process terms cardiovascular system development and extracellular matrix. Data are presented as a heat map of relative over- and under-expression in rosiglitazone treated with respect to control DMSO treated NRVMs (Figure 6). Q-PCR was carried out as described previously [36]. This revealed that these transcripts were progressively upregulated as the time course proceeded and validated the array data.

Discussion

Recently, the Type 2 diabetes medication, rosiglitazone, has come under scrutiny for its potential to cause myocardial ischemia [15]. Existing data on the cardiovascular effects of PPAR-γ agonists including rosiglitazone are conflicting. Several studies suggest an increased risk of cardiovascular events. Other studies indicate cardioprotective effects and improvement in myocardial function. To date, few studies have examined global cardiac gene-expression changes resulting from rosiglitazone treatment. One investigated the effects of rosiglitazone on the diabetic heart using cardiac transcriptional profiling and imaging studies of a murine model of Type 2 diabetes, the C57BL/KLS-leprdb/leprdb (db/db) mouse [37]. Cardiac gene-expression profiles were compared across three groups of untreated db/db mice, db/db mice after rosiglitazone treatment and non-diabetic db/+ mice. In parallel cardiac magnetic resonance and echocardiography studies were carried out. The authors noted that the db/db gene-expression signature was not significantly reversed with rosiglitazone treatment. More troubling however was the fact that a number of rosiglitazone

modulated genes and pathways that may play a role in the pathophysiology of the increase in cardiac mortality were uncovered.

In order to explore the temporal effects of rosiglitazone on cardiac gene expression we utilized a well established neonatal rat cardiomyocyte model coupled to a single dose of the drug. The rationale for the single dose selection was based on cost considerations, and the fact that previous work has indicated cardioprotective effects of the drug at (10 μmol/l) [17]. The NRVM primary cell was selected over established cell lines as it represents a well recognized model for morphological, biochemical and electrophysiological analyses. Additionally NRVMs facilitate a broad spectrum of analyses including contraction, ischemia, hypoxia and drug transport and toxicity studies [24,25]. We examined temporal differences in gene expression between exposed and control cells across a 48 h window using an Illumina whole-genome rat microarray.

Our analysis consisted initially of examining changes in gene expression across the entire course. This revealed that the GO terms lipid metabolic process, response to lipid and immune response were significantly enriched (Figures 1 & 2). These are well established responses to rosiglitazone and their enrichment in the exposed NRVMs provided confidence in the experimental approach and the quality of the microarray data. Many of the transcripts involved in immune responses were downregulated suggesting that inflammation may not be the cause of the adverse cardiac outcomes associated with the drug (Figure 2). Previous work revealed that in the absence of an inflammatory signal rosiglitazone exhibited no significant effects on basal levels of NF-κB-dependent transcription and IL-6 secretion [17]. The anti-inflammatory effects suggest a potential cardioprotective role for rosiglitazone treatment that may be therapeutically beneficial for the treatment of T2DM.

Lipid metabolic processes

We selected a series of key transcripts involved in lipid metabolic processes (*ANGPTL4, ECH1, HMGCS2, CPT1A* and *CYP1B1*) that were significantly upregulated for validation by Q-PCR (Figure 6). This revealed that the expression patterns obtained using both platforms concurred with significant upregulation of these transcripts, all of which increased with the exposure time.

The transcript that exhibited the greatest change in expression in response to rosiglitazone was *ANGPTL4*, which plays a critical role in modulating cardiac substrate metabolism. *ANGPTL4* is activated by all PPAR family ligands [38]. *ANGPTL4* overexpression has been linked with detrimental cardiac effects. It is a potent inhibitor of lipoprotein lipase (LPL), regulating its activity in adipose, hepatic and cardiac tissue. In cardiac myocytes, LPL hydrolyses lipoproteins generating free fatty acids (FFA), which are oxidized to produce ATP [39]. As the heart relies predominately on lipoprotein-derived FFA as its primary fuel source, loss of LPL-derived FFA by ANGPTL4 leads to cardiac dysfunction and impaired contractility [40].

Another consistently upregulated transcript was *ECH1*, a PPAR-responsive gene encoding a protein that is involved in peroxisomal β-oxidation. *ECH1* has been implicated along with the ability of peroxisomes to oxidize long-chain fatty acids as a cardiac substrate for energy

production [41,42]. *HMGCS2* was strongly upregulated during the rosiglitazone time course. *HMGCS2* is a PPAR-α regulated gene and the mitochondrial form is responsible for the biosynthesis of ketone bodies. The observation that *HMGCS2* is upregulated and increases steadily with time, indicates a longer lag time in the production of ketone bodies relative to the time required for the mitochondria to absorb and oxidize fatty acids for energy consumption. Although they play a minor role, ketone bodies serve as a minor energy substrate for the myocardium under normal conditions. However, during starvation or poorly controlled diabetes for example, plasma ketone body levels have been found to increase. When they are oxidized for ATP production, this inhibits fatty acid β-oxidation causing a net decrease in the rate of ATP production for the working heart [43]. Cardiac failure in T2DM patients has been associated with elevated plasma ketone body formation. It is interesting therefore to speculate that upregulated *HMGCS2* expression pattern may serve as an indicator variable for heart failure in T2DM patients.

CYP1B1 belongs to the CYP450 superfamily of enzymes responsible for drug metabolism and detoxification of toxic chemicals [44]. Rosiglitazone treatment upregulated *CYP1B1* mRNA. The role of CYP450 in cardiovascular health and disease is well established. Many CYP450 enzymes have been identified in the heart and their mRNA and enzymatic levels (including CYP1B) have been reported to be increased during cardiac hypertrophy and heart failure [45].

CPT1 is a mitochondrial enzyme belonging to the carnitine acyltransferase family. *CPT1A*, one of three known isoforms was strongly upregulated in response to rosiglitazone. CPT1 functions by mediating transport of long-chain fatty acids across the mitochondrial membrane and consequently has significance in metabolic disorders such as diabetes where FFA levels become elevated, fats accumulate in skeletal muscle, and muscular tissue has a decreased ability to oxidize fatty acids. CPT1 has been implicated in playing a critical role in the development of these symptoms in metabolic diseases [46–48].

Immediate, intermediate & late gene-expression profiles

Our analysis also consisted of exploring groups of transcripts that were collectively modulated in response to rosiglitazone. We stratified the data set into three different stages, representing immediate, intermediate and late gene-expression profiles (Figure 3). The rationale for this approach was that even though there were different time points present in each stage, we speculated that the relevant biological processes that were altered were continuous in time, and that the rank of the impacted genes at these time points within one group remained the same within the group. This facilitated discovery of transcripts that were consistently expressed in response to the drug, yet masked when the time course data was analyzed in its entirety due to the magnitude of the ‘lipid metabolism’ and immune response responses.

Two significant GO terms that were uncovered using this approach were extracellular matrix cellular component and cardiovascular system development biological process both of which point to adverse cardiac outcomes. We also noted the appearance of the term ‘programmed cell death’ in stage III (Figure 3), which upon initial analysis suggested that the rosiglitazone treated cells were undergoing apoptosis. A limitation of this study was that the approach

employed did not facilitate extensive phenotypic analysis of the cells over time. However rosiglitazone treatment decreased cell size progressively with increased exposure time, early (stage I) by 16%; mid (stage II) by 11%; and late (stage III) by 36%. This media used for cell culture was essentially a starvation medium. A likely explanation for the appearance of this term late in the time course is the cellular response to the prolonged period the primary cells have spent in culture.

Cardiovascular system development

Heart and vascular system development commences early in mesoderm. Many of the transcripts pertinent to cardiovascular system development were modulated by exposure to rosiglitazone in NRVMs, suggesting that their inappropriate expression in response to the drug may contribute to adverse cardiac outcomes (Figure 4). In addition to *Angptl4*, described above, transcripts belonging to the GO biological process term cardiovascular system development included *ALPK3, BMPR1A, Cdc42, Cathepsin H, Hopx, JAG1* and *JPH2* (Figure 3).

ALPK3 a nuclear kinase involved in the differentiation of cardiomyocytes was upregulated in the immediate and late stages, but down-regulated in the intermediate stage. Cardiomyopathy has been described in mice deficient for *ALPK3* [49]. *BMPR1A* bone morphogenetic protein receptor was upregulated in the immediate and late stages. Bone morphogenetic protein (BMP) signaling is involved in the regulation of cell proliferation, migration, differentiation and apoptosis, through binding of BMPs to a heterodimeric complex of two transmembrane receptors, termed BMPR type I and type II. Clinical and molecular data both point towards a key role for *BMPR1A* in the genesis of congenital heart defects [50]. A cardiac-specific deletion of *BMPR1A* disrupted cardiac morphogenesis in mice, with ventricular septum, trabeculation and endocardial cushion defects present [51].

Cdc42 was upregulated in the immediate and intermediate stages and downregulated in the late stage. Cdc42 functions as an antihypertrophic molecular switch in the heart. Mice with a heart-specific deletion of *Cdc42* were found to develop greater cardiac hypertrophy at 2 and 8 weeks of stimulation and transitioned more quickly into heart failure than did wild-type controls [52]. *Cathepsin H*, which encodes a lysosomal cysteine proteinase involved in the degradation of lysosomal proteins was downregulated in the rosiglitazone treated myocytes. Cathepsin expression and activity has been extensively documented in both failing cardiac tissues and in cultured cardiomyocytes [53].

Hopx exhibits diverse effects on cardiac growth. *Hopx* loss of function studies in murine models resulted in cardiac hypertrophy, dilation and fibrosis. *Hopx* expression was diminished in both human and murine cardiac hypertrophy and failure [54]. In rosiglitazone exposed myocytes, *Hopx* was upregulated in the immediate and intermediate stages and downregulated in the late stage.

Mutations in *JAG1*, a conserved member of the Notch intercellular signaling pathway, cause Alagille syndrome, an autosomal dominant disorder characterized by developmental abnormalities in the heart, and additionally in the liver, eye, skeleton and kidney [55]. In the

rosiglitazone exposed NRVMs *JAG1* expression was upregulated in the immediate stage and downregulated in the intermediate and late stages.

JPH2, belongs to the junctophilin gene family (the other members of the family are *JPH1*, *JPH3* and *JPH4*). *JPH2* was upregulated in the immediate stage and its expression fluctuated in the intermediate and late stages in drug treated myocytes. *JPH2* is the predominant isoform in cardiac tissue. Mutations in *JPH2* were identified in a cohort of patients with hypertrophic cardiomyopathy. *JPH2* was found to be downregulated in several animal models of heart failure [56,57].

Extracellular matrix

The extracellular matrix is a macromolecular complex, comprised of collagens, elastic fibers, proteoglycans and basement membranes [58]. It forms a structural network for transmitting force generated by individual myocytes into the organized systolic contraction of the heart. In addition to structural functions, extracellular matrix components also serve as modulators of growth, tissue differentiation and angiogenesis [59]. Rosiglitazone treatment resulted in disruption in the normal expression patterns of many extracellular matrix proteins in NRVMs and this perturbation may contribute to the adverse cardiac outcomes reported with this drug (Figure 5).

Increased basal levels of extracellular matrix degradation have been attributed to the development of cardiomyopathy in collagen I mutant mice [60]. Careful study of collagen I mutant mice revealed that turnover of extracellular matrix components is strongly interwoven and alterations in extracellular matrix composition may provoke cardiac dysfunction [58]. An important characteristic of hypertrophy and heart failure is cardiac fibrosis, which is characterized by an increase in collagens and other extracellular matrix components in the interstitium and perivascular regions of the myocardium [61]. Excessive production of extracellular matrix proteins increases myocardial stiffness, thereby altering cardiac mechanics, and contributing to the pathophysiology of heart failure.

The activity of matrix metalloproteinases (MMPs) is negligible in normal steady-state tissues. MMP expression is modulated by inflammatory cytokines, growth factors, hormones, cell–cell and cell–matrix interaction [62,63]. MMP activities are also regulated by activation of precursor zymogens and inhibition by endogenous inhibitors, the tissue inhibitors of metalloproteinases (TIMPs). Thus, homeostasis between MMPs and TIMPs is critical for extracellular matrix remodeling in cardiac tissue. An interesting observation in the data set is that rosiglitazone exposure caused overexpression of *Timp1* and downregulation of *Mmp12*. Timp1 is an inhibitor of Mmp12, which functions in the breakdown of extracellular matrix in normal physiological processes [62]. *Mmp9* and *Mmp14* also exhibited differential expression profiles in response to rosiglitazone. *Mmp14* expression was increased during stage I and subsequently decreased for the remainder of the time course. *MMP-9* activity was upregulated initially in response to rosiglitazone treatment and as the time of exposure progressed was downregulated. *MMP-9* induction has been noted in the mouse heart subjected to ischemic insult. Studies using an *Mmp9* gene knockout mice have indicated that *Mmp9* plays a key role in cardiac rupture following myocardial infarction [64]. A critical role for *MMP-9*, working in concert with another

family member *MMP-2*, has been the development of abdominal aortic aneurysm [65]. Both *MMP-2* and *MMP-9* cleave elastin, type IV collagen, and several other extracellular matrix molecules and MMP-2 digests interstitial collagen types I, II and III.

Additional extracellular matrix components whose expression was modulated by rosiglitazone, included *ADAMTS7* and *ADAMTS9*, which encode secreted zinc metalloproteinases. *ADAMTS7* was downregulated by exposure to the drug. Studies in animal models have revealed that ADAMTS7 functions in neointima formation after arterial mechanical injury, by facilitating vascular smooth muscle cell migration. Recent human genome-wide analysis studies have uncovered an association between DNA polymorphisms at the *ADAMTS7* gene locus and coronary artery disease risk [66,67]. *ADAMTS9* was upregulated in response to rosiglitazone. An *ADAMTS9* gene variant associated with Type 2 diabetes was identified in the 5′-upstream region. This allele resulted in reduced insulin-stimulated glucose uptake [68]. The molecular mechanisms underlying the effect of *ADAMTS9* on peripheral insulin action, risk of diabetes and adverse cardiac outcomes, however, are unknown.

Cardiac fibroblasts are the most prominent cell type in the mammalian heart, comprising 60–70% of the cells. They function in regulating normal myocardial function and in the adverse myocardial remodeling associated with myocardial infarction and heart failure [69]. Commonly prescribed therapeutics including rosiglitazone, exert pleiotropic effects on cardiac fibroblasts. Although the purity of the NRVM enrichment is >99%, given the sensitivity of the data analysis approach we employed, it is possible that the effects of rosiglitazone on the normal expression of extracellular matrix proteins observed was due to residual cardiac fibroblasts in culture.

Conclusion

In summary, the genome-wide expression data and systems level analysis reported here indicate that there are biomarkers associated with both beneficial and adverse cardiac effects in response to rosiglitazone exposure. We uncovered several mechanisms and parallel avenues through which negative cardiac outcomes could be mediated including lipid metabolic processes and extracellular matrix components. A limitation of this study was that the biomarkers related to cardioprotective and/or cardiac dysfunctional processes mediated through the actions of rosglitazone were uncovered solely via genomic and bioinformatics analyses. We provide a series of biomarkers for rosiglitazone exposure and adverse outcomes that can be further investigated in animal and human models. This will be the subject of future work.

Supplementary Material

Refer to Web version on PubMed Central for supplementary material.

Acknowledgments

The authors thank R Šášik and the UCSD Biomedical Genomics Facility for help with microarray data analysis. The authors are grateful to V Nigam and past and present members of the Paolini and Hardiman laboratories for useful discussions.

This work was carried out in the Paolini (ppaolini@sunstroke.sdsu.edu) and Hardiman (hardiman@musc.edu) laboratories. G Hardiman acknowledges support from NIH grants DK063491, CA023100 and DK080506. P Paolini acknowledges support from the Computational Science Research Center and a grant from the California Metabolic Research Foundation.

References

1. Threatt J, Williamson JF, Huynh K, Davis RM. Ocular disease, knowledge and technology applications in patients with diabetes. Am. J. Med. Sci. 2013; 345(4):266–270. [PubMed: 23531956]
2. Zhang P, Zhang X, Brown J, et al. Global healthcare expenditure on diabetes for 2010 and 2030. Diabetes Res. Clin. Pract. 2010; 87(3):293–301. [PubMed: 20171754]
3. Spiegelman BM. PPAR-gamma: adipogenic regulator and thiazolidinedione receptor. Diabetes. 1998; 47(4):507–514. [PubMed: 9568680]
4. Krentz AJ, Bailey CJ. Oral antidiabetic agents: current role in Type 2 diabetes mellitus. Drugs. 2005; 65(3):385–411. [PubMed: 15669880]
5. Gerstein HC, Yusuf S. DREAM (Diabetes REduction Assessment with ramipril and rosiglitazone Medication) Trial Investigators. Effect of rosiglitazone on the frequency of diabetes in patients with impaired glucose tolerance or impaired fasting glucose: a randomised controlled trial. Lancet. 2006; 368(9541):1096–1105. [PubMed: 16997664]
6. Vasan RS, Sullivan LM, Roubenoff R, et al. Inflammatory markers and risk of heart failure in elderly subjects without prior myocardial infarction: the Framingham Heart Study. Circulation. 2003; 107(11):1486–1491. [PubMed: 12654604]
7. Khandoudi N, Delerive P, Berrebi-Bertrand I, Buckingham RE, Staels B, Bril A. Rosiglitazone, a peroxisome proliferator-activated receptor-gamma, inhibits the Jun NH(2)-terminal kinase/activating protein 1 pathway and protects the heart from ischemia/reperfusion injury. Diabetes. 2002; 51(5):1507–1514. [PubMed: 11978649]
8. Nissen SE, Wolski K. Effect of rosiglitazone on the risk of myocardial infarction and death from cardiovascular causes. N. Engl. J. Med. 2007; 356(24):2457–2471. [PubMed: 17517853]
9. Bell DS, Ovalle F. Tissue triglyceride levels in Type 2 diabetes and the role of thiazolidinediones in reversing the effects of tissue hypertriglyceridemia: review of the evidence in animals and humans. Endocrine Pract. 2001; 7(2):135–138.
10. Ovalle F, Bell D. Lipoprotein effects of different thiazolidinediones in clinical practice. Endocrine Pract. 2002; 8(6):406–410.
11. Nemoto S, Razeghi P, Ishiyama M, De Freitas G, Taegtmeyer H, Carabello BA. PPAR-gamma agonist rosiglitazone ameliorates ventricular dysfunction in experimental chronic mitral regurgitation. Am. J. Physiol. Heart Circ. Physiol. 2005; 288(1):H77–H82. [PubMed: 15345480]
12. Grundy SM, Benjamin IJ, Burke GL, et al. Diabetes and cardiovascular disease: a statement for healthcare professionals from the American Heart Association. Circulation. 1999; 100(10):1134–1146. [PubMed: 10477542]
13. Home P. Cardiovascular disease and oral agent glucose-lowering therapies in the management of Type 2 diabetes. Diabetes Technol. Ther. 2012; 14(Suppl. 1):S33–S42. [PubMed: 22650223]
14. Ajjan RA, Grant PJ. The cardiovascular safety of rosiglitazone. Expert Opin. Drug Saf. 2008; 7(4):367–376. [PubMed: 18613801]
15. Rosen CJ. Revisiting the rosiglitazone story – lessons learned. N. Engl. J. Med. 2010; 363(9):803–806. [PubMed: 20660395]
16. Blind E, Dunder K, De Graeff PA, Abadie E. Rosiglitazone: a European regulatory perspective. Diabetologia. 2011; 54(2):213–218. [PubMed: 21153629]
17. Shah RD, Gonzales F, Golez E, et al. The antidiabetic agent rosiglitazone upregulates SERCA2 and enhances TNF-alpha- and LPS-induced NF-kappaB-dependent transcription and TNF-alpha-induced IL-6 secretion in ventricular myocytes. Cell. Physiol. Biochem. 2005; 15(1–4):41–50. [PubMed: 15665514]
18. Auwerx J. PPARgamma, the ultimate thrifty gene. Diabetologia. 1999; 42(9):1033–1049. [PubMed: 10447513]

19. Desvergne B, Wahli W. Peroxisome proliferator-activated receptors: nuclear control of metabolism. Endocrine Rev. 1999; 20(5):649–688. [PubMed: 10529898]
20. Gilde AJ, van Bilsen M. Peroxisome proliferator-activated receptors (PPARS): regulators of gene expression in heart and skeletal muscle. Acta Physiol. Scand. 2003; 178(4):425–434. [PubMed: 12864748]
21. Robinson E, Grieve DJ. Significance of peroxisome proliferator-activated receptors in the cardiovascular system in health and disease. Pharmacol. Ther. 2009; 122(3):246–263. [PubMed: 19318113]
22. von Bibra H, Diamant M, Scheffer PG, Siegmund T, Schumm-Draeger PM. Rosiglitazone, but not glimepiride, improves myocardial diastolic function in association with reduction in oxidative stress in Type 2 diabetic patients without overt heart disease. Diabetes Vasc. Dis. Res. 2008; 5(4): 310–318.
23. Psaty BM, Furberg CD. Rosiglitazone and cardiovascular risk. N. Engl. J. Med. 2007; 356(24): 2522–2524. [PubMed: 17517854]
24. Chlopcikova S, Psotova J, Miketova P. Neonatal rat cardiomyocytes – a model for the study of morphological, biochemical and electrophysiological characteristics of the heart. Biomed. Pap. Med. Fac. Univ. Palacky Olomouc Czech. Repub. 2001; 145(2):49–55. [PubMed: 12426771]
25. Wenzel DG, Wheatley JW, Byrd GD. Effects of nicotine on cultured rat heart cells. Toxicol. Appl. Pharmacol. 1970; 17(3):774–785. [PubMed: 4395627]
26. Sasik R, Woelk CH, Corbeil J. Microarray truths and consequences. J. Mol. Endocrinol. 2004; 33(1):1–9. [PubMed: 15291738]
27. Benjamini Y, Hochberg Y. Controlling the false discovery rate: a practical and powerful approach to multiple testing. J. Royal Stat. Soc. Series B (Methodological). 1995; 57(1):289–300.
28. Tusher VG, Tibshirani R, Chu G. Significance analysis of microarrays applied to the ionizing radiation response. Proc. Natl Acad. Sci. USA. 2001; 98(9):5116–5121. [PubMed: 11309499]
29. The R Project for Statistical Computing www.r-project.org
30. R Development Core TeamR: a language and environment for statistical computing R Foundation for Statistical Computing; Vienna, Austria: 2008
31. Olds EG. A note on the convolution of uniform distributions. Ann. Math. Stat. 1952; 23(2):282–285.
32. Subramanian A, Tamayo P, Mootha VK, et al. Gene set enrichment analysis: a knowledge-based approach for interpreting genome-wide expression profiles. Proc. Natl Acad. Sci. USA. 2005; 102(43):15545–15550. [PubMed: 16199517]
33. Meilă M. Comparing clusterings by the variation of information. Learn. Theory Kernel Machines. 2003; 2777:173–187.
34. Meilă M. Comparing clusterings – an information based distance. J. Multivariate Anal. 2007; 98(5):873–895.
35. Jiang H, Wong WH. SeqMap: mapping massive amount of oligonucleotides to the genome. Bioinformatics. 2008; 24(20):2395–2396. [PubMed: 18697769]
36. Baker ME, Ruggeri B, Sprague LJ, et al. Analysis of endocrine disruption in Southern California coastal fish using an aquatic multispecies microarray. Environ. Health Perspect. 2009; 117(2):223–230. [PubMed: 19270792]
37. Wilson KD, Li Z, Wagner R, et al. Transcriptome alteration in the diabetic heart by rosiglitazone: implications for cardiovascular mortality. PLoS ONE. 2008; 3(7):e2609. [PubMed: 18648539]
38. Sukonina V, Lookene A, Olivecrona T, Olivecrona G. Angiopoietin-like protein 4 converts lipoprotein lipase to inactive monomers and modulates lipase activity in adipose tissue. Proc. Natl Acad. Sci. USA. 2006; 103(46):17450–17455. [PubMed: 17088546]
39. Augustus AS, Buchanan J, Park TS, et al. Loss of lipoprotein lipase-derived fatty acids leads to increased cardiac glucose metabolism and heart dysfunction. J. Biol. Chem. 2006; 281(13):8716–8723. [PubMed: 16410253]
40. Yu X, Burgess SC, Ge H, et al. Inhibition of cardiac lipoprotein utilization by transgenic overexpression of Angptl4 in the heart. Proc. Natl Acad. Sci. USA. 2005; 102(5):1767–1772. [PubMed: 15659544]

41. Fitzpatrick DR, Germain-Lee E, Valle D. Isolation and characterization of rat and human cDNAs encoding a novel putative peroxisomal enoyl-CoA hydratase. Genomics. 1995; 27(3):457–466. [PubMed: 7558027]
42. Barger PM, Kelly DP. PPAR signaling in the control of cardiac energy metabolism. Trends Cardiovasc. Med. 2000; 10(6):238–245. [PubMed: 11282301]
43. Stanley WC, Recchia FA, Lopaschuk GD. Myocardial substrate metabolism in the normal and failing heart. Physiol. Rev. 2005; 85(3):1093–1129. [PubMed: 15987803]
44. Sprenkle AB, Murray SF, Glembotski CC. Involvement of multiple *cis* elements in basal- and alpha-adrenergic agonist-inducible atrial natriuretic factor transcription. Roles for serum response elements and an SP-1-like element. Circ. Res. 1995; 77(6):1060–1069. [PubMed: 7586217]
45. Zordoky BN, El-Kadi AO. Modulation of cardiac and hepatic cytochrome P450 enzymes during heart failure. Curr. Drug Metabol. 2008; 9(2):122–128.
46. Bonnefont JP, Djouadi F, Prip-Buus C, Gobin S, Munnich A, Bastin J. Carnitine palmitoyltransferases 1 and 2: biochemical, molecular and medical aspects. Mol. Aspects Med. 2004; 25(5–6):495–520. [PubMed: 15363638]
47. van der Leij FR, Huijkman NC, Boomsma C, Kuipers JR, Bartelds B. Genomics of the human carnitine acyltransferase genes. Mol. Genet. Metabol. 2000; 71(1–2):139–153.
48. Rasmussen BB, Holmbäck UC, Volpi E, Morio-Liondore B, Paddon-Jones D, Wolfe RR. Malonyl coenzyme A and the regulation of functional carnitine palmitoyltransferase-1 activity and fat oxidation in human skeletal muscle. J. Clin. Invest. 2002; 110(11):1687–1693. [PubMed: 12464674]
49. van Sligtenhorst I, Ding ZM, Shi ZZ, Read RW, Hansen G, Vogel P. Cardiomyopathy in alpha-kinase 3 (ALPK3)-deficient mice. Vet. Pathol. 2012; 49(1):131–141. [PubMed: 21441111]
50. Breckpot J, Tranchevent LC, Thienpont B, et al. BMPR1A is a candidate gene for congenital heart defects associated with the recurrent 10q22q23 deletion syndrome. Eur. J. Med. Genet. 2012; 55(1):12–16. [PubMed: 22067610]
51. Gaussin V, van de Putte T, Mishina Y, et al. Endocardial cushion and myocardial defects after cardiac myocyte-specific conditional deletion of the bone morphogenetic protein receptor ALK3. Proc. Natl Acad. Sci. USA. 2002; 99(5):2878–2883. [PubMed: 11854453]
52. Maillet M, Lynch JM, Sanna B, York AJ, Zheng Y, Molkentin JD. Cdc42 is an antihypertrophic molecular switch in the mouse heart. J. Clin. Invest. 2009; 119(10):3079–3088. [PubMed: 19741299]
53. Cheng XW, Shi GP, Kuzuya M, Sasaki T, Okumura K, Murohara T. Role for cysteine protease cathepsins in heart disease: focus on biology and mechanisms with clinical implication. Circulation. 2012; 125(12):1551–1562. [PubMed: 22451605]
54. Trivedi CM, Cappola TP, Margulies KB, Epstein JA. Homeodomain only protein x is down-regulated in human heart failure. J. Mol. Cell Cardiol. 2011; 50(6):1056–1058. [PubMed: 21382376]
55. Loomes KM, Underkoffler LA, Morabito J, et al. The expression of Jagged1 in the developing mammalian heart correlates with cardiovascular disease in Alagille syndrome. Hum. Mol. Genet. 1999; 8(13):2443–2449. [PubMed: 10556292]
56. Landstrom AP, Weisleder N, Batalden KB, et al. Mutations in JPH2-encoded junctophilin-2 associated with hypertrophic cardiomyopathy in humans. J. Mol. Cell. Cardiol. 2007; 42(6):1026–1035. [PubMed: 17509612]
57. Garbino A, van Oort RJ, Dixit SS, Landstrom AP, Ackerman MJ, Wehrens XH. Molecular evolution of the junctophilin gene family. Physiol. Genomics. 2009; 37(3):175–186. [PubMed: 19318539]
58. Creemers EE, Pinto YM. Molecular mechanisms that control interstitial fibrosis in the pressure-overloaded heart. Cardiovasc. Res. 2011; 89(2):265–272. [PubMed: 20880837]
59. Weber KT, Sun Y, Tyagi SC, Cleutjens JP. Collagen network of the myocardium: function, structural remodeling and regulatory mechanisms. J. Mol. Cell. Cardiol. 1994; 26(3):279–292. [PubMed: 8028011]
60. Miller AD, Tyagi SC. Mutation in collagen gene induces cardiomyopathy in transgenic mice. J. Cell. Biochem. 2002; 85(2):259–267. [PubMed: 11948682]

61. Berk BC, Fujiwara K, Lehoux S. ECM remodeling in hypertensive heart disease. J. Clin. Invest. 2007; 117(3):568–575. [PubMed: 17332884]

62. Nagase H, Visse R, Murphy G. Structure and function of matrix metalloproteinases and TIMPs. Cardiovasc. Res. 2006; 69(3):562–573. [PubMed: 16405877]

63. Nagase H, Woessner JF. Matrix metalloproteinases. J. Biol. Chem. 1999; 274(31):21491–21494. [PubMed: 10419448]

64. Romanic AM, Harrison SM, Bao W, et al. Myocardial protection from ischemia/ reperfusion injury by targeted deletion of matrix metalloproteinase-9. Cardiovasc. Res. 2002; 54(3):549–558. [PubMed: 12031700]

65. Longo GM, Xiong W, Greiner TC, Zhao Y, Fiotti N, Baxter BT. Matrix metalloproteinases 2 and 9 work in concert to produce aortic aneurysms. J. Clin. Invest. 2002; 110(5):625–632. [PubMed: 12208863]

66. Reilly MP, Li M, He J, et al. Identification of ADAMTS7 as a novel locus for coronary atherosclerosis and association of ABO with myocardial infarction in the presence of coronary atherosclerosis: two genome-wide association studies. Lancet. 2011; 377(9763):383–392. [PubMed: 21239051]

67. Patel RS, Ye S. ADAMTS7: a promising new therapeutic target in coronary heart disease. Expert Opin. Ther. Targets. 2013; 17(8):863–867. [PubMed: 23829786]

68. Boesgaard TW, Gjesing AP, Grarup N, et al. Variant near ADAMTS9 known to associate with Type 2 diabetes is related to insulin resistance in offspring of Type 2 diabetes patients – EUGENE2 study. PLoS ONE. 2009; 4(9):e7236. [PubMed: 19789630]

69. Porter KE, Turner NA. Cardiac fibroblasts: at the heart of myocardial remodeling. Pharmacol. Ther. 2009; 123(2):255–278. [PubMed: 19460403]

Executive summary

Objective

- Cardiovascular disease remains the leading cause of death among diabetic patients. Despite the proven anti-inflammatory and insulin sensitizing properties of rosiglitazone, the literature regarding rosiglitazone and ischemic cardiovascular risk is conflicting. Because of the pleiotropic effects of rosiglitazone as a PPAR-γ agonist, uncovering the precise cellular and molecular mechanisms that may contribute to adverse cardiac responses has been challenging.

Approach

- In this study, a systems approach was used to investigate the effects of rosiglitazone (Avandia®) exposure on genome-wide gene expression in a well established cardiac cell model, neonatal rat ventricular myocytes. This revealed that the gene ontology terms ‘lipid metabolic process’, ‘response to lipid’ and ‘immune response’ were significantly enriched.
- A series of transcripts involved in lipid metabolic processes (*ANGPTL4, ECH1, HMGCS2, CPT1A* and *CYP1B1*) that were significantly upregulated were validated using quantitative PCR. Significant upregulation of these transcripts was observed, which increased with drug exposure time.
- To better elucidate the temporal effects of rosiglitazone exposure, the data was stratified into three different groups, representing immediate, intermediate and late gene-expression profiles.
- This approach facilitated discovery of transcripts that were consistently expressed in response to the drug, yet masked when the time course data was analyzed in its entirety owing to the magnitude of the ‘lipid metabolism’ and ‘immune response’ responses.
- Two significant gene ontology terms that were uncovered using this approach were ‘extracellular matrix’ cellular component and ‘cardiovascular system development’ biological process, both of which point to adverse cardiac outcomes.

Conclusion

- The systems level analysis reported here indicate that there are biomarkers associated with both beneficial and adverse cardiac effects in response to rosiglitazone exposure. Several mechanisms and parallel avenues through which negative cardiac outcomes could be mediated were uncovered. This series of biomarkers can be further investigated in animal and human models.

Figure 1. Heat map of gene-expression changes in neonatal rat ventricular myocytes in response to rosiglitazone involving transcripts that play a role in lipid metabolism

Red and blue colored boxes depict relative over- and under-expression in rosiglitazone treated with respect to control DMSO treated neonatal rat ventricular myocytes. The range of colors is between −4-fold and +4-fold and preserves qualitative relationships among individual values. All fold changes outside of this range have been truncated to ±4. Genes found significant at the level $q < 0.05$ in the entire time course comparison are shown.

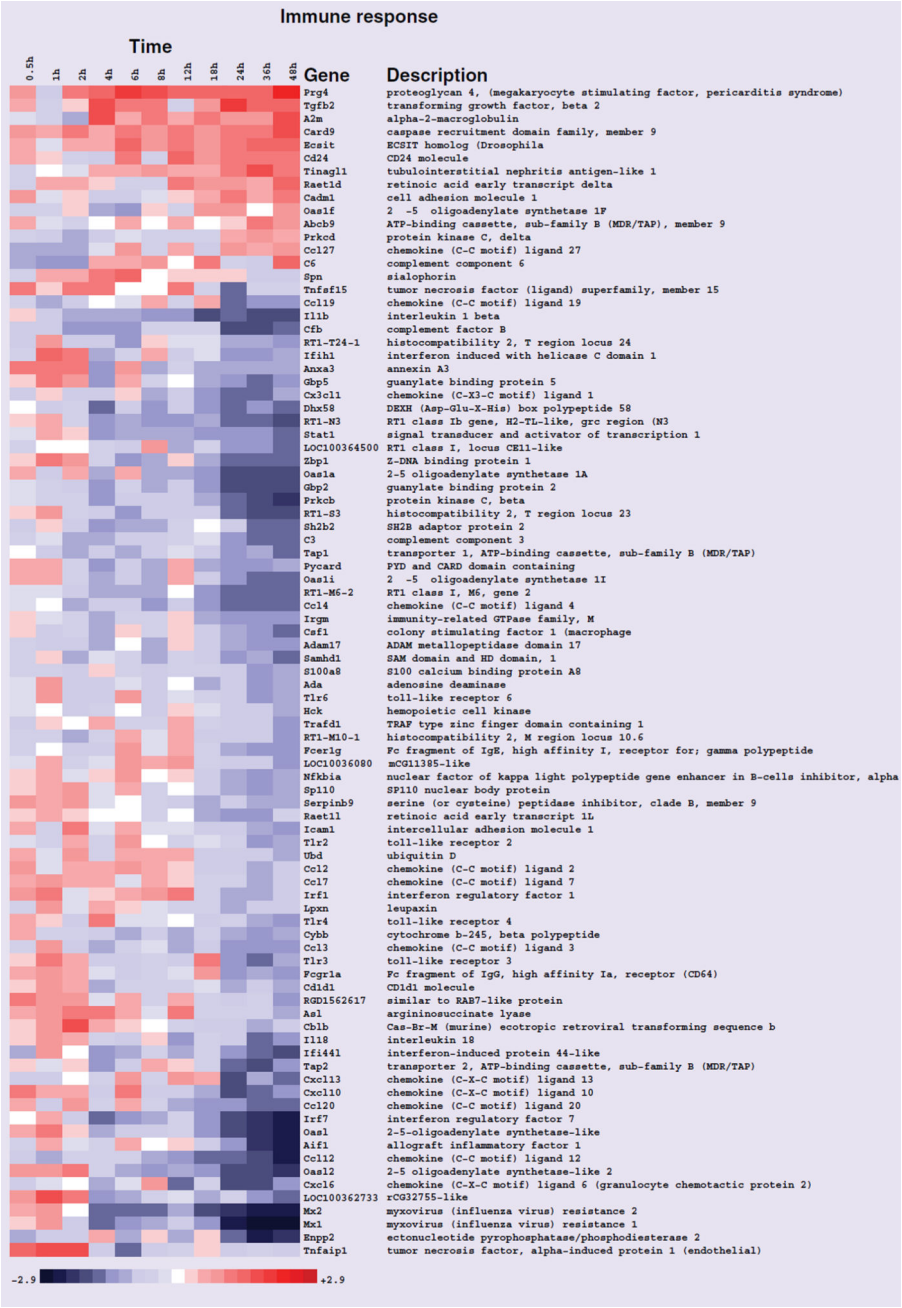

Figure 2. Heat map of gene-expression changes in neonatal rat ventricular myocytes in response to rosiglitazone involving transcripts that function in immune response

Red and blue colored boxes depict relative over- and under-expression in rosiglitazone treated with respect to control DMSO treated neonatal rat ventricular myocytes. The range of colors is between −2.9-fold and +2.9-fold and preserves qualitative relationships among individual values. Genes found significant at the level $q < 0.05$ in the entire time course comparison are shown.

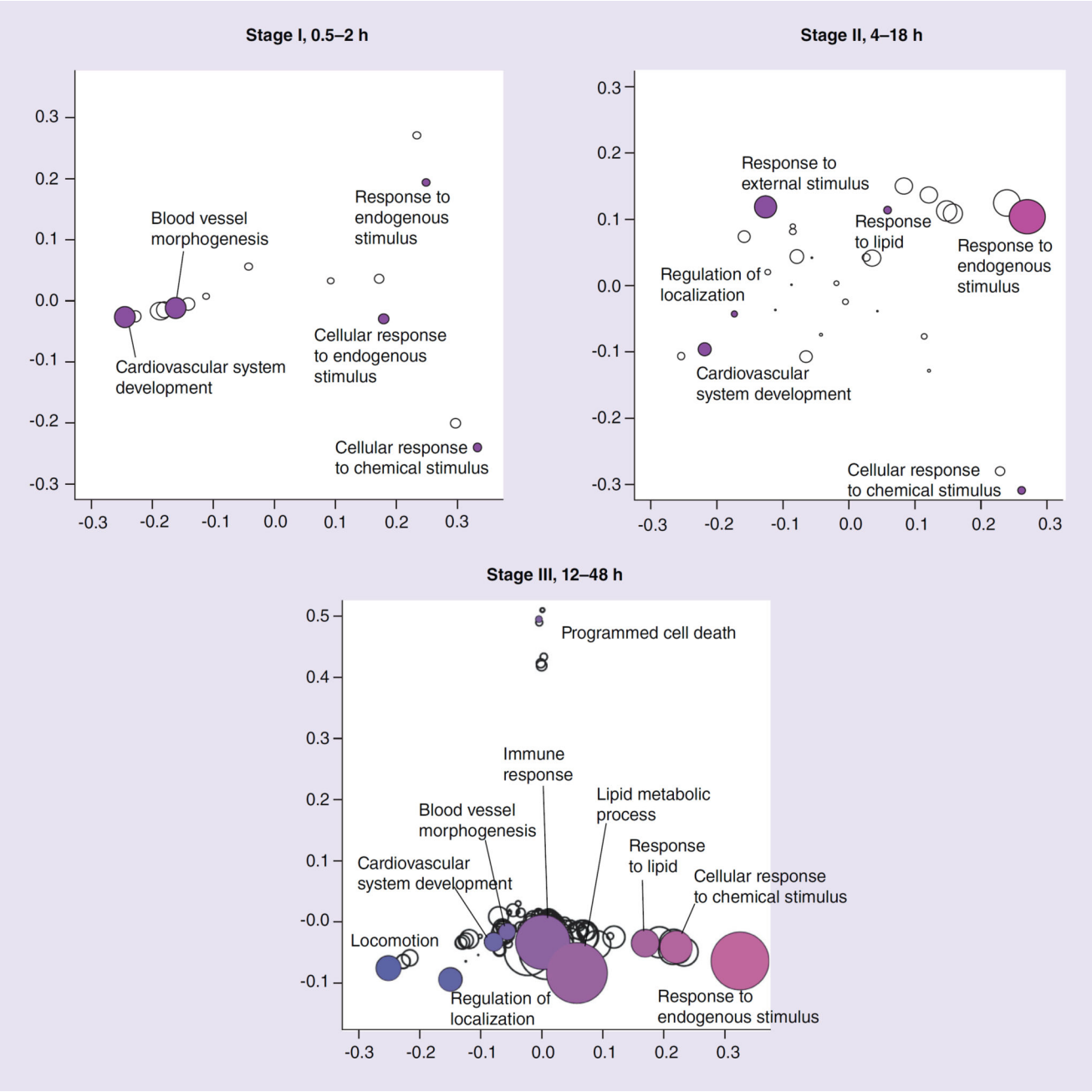

Figure 3. Information clustering of biological processes found to be significant (Bonferroni p-value <0.01) in stages I, II and III

Distance between symbols reflects variability of information between terms. Symbol size is proportional to statistical significance of terms; larger symbols infer greater significance. Colors have no significance and are used merely for greater legibility.

Figure 4. Heat map of gene-expression changes in neonatal rat ventricular myocytes in response to rosiglitazone involving transcripts that function in cardiovascular system development

Red and blue colored boxes depict relative over- and under-expression in rosiglitazone treated with respect to control DMSO treated neonatal rat ventricular myocytes at the time points indicated. The range of colors is between −4-fold and +4-fold and preserves qualitative relationships among values. All fold changes outside of this range have been truncated to ±4. Genes found significant at the level $q < 0.2$ in stage I (0.5–2 h) are shown.

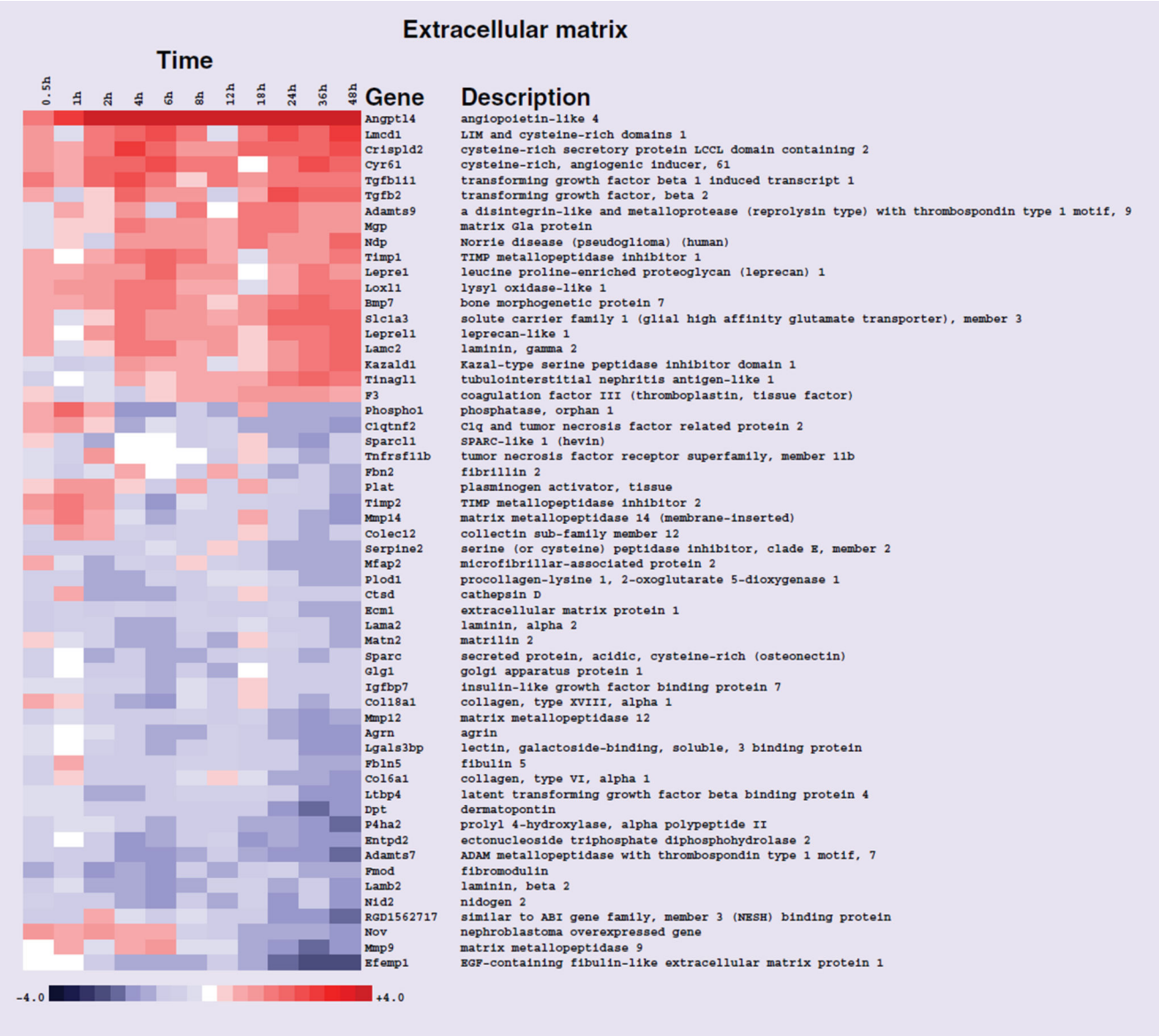

Figure 5. Heat map of gene-expression changes in neonatal rat ventricular myocytes in response to rosiglitazone involving transcripts that function in the extracellular matrix cellular component

Red and blue colored boxes depict relative over- and under-expression in rosiglitazone treated with respect to control DMSO treated neonatal rat ventricular myocytes. The range of colors is between −4-fold and +4-fold and preserves qualitative relationships among individual values. All fold changes outside of this range have been truncated to ±4. Genes found significant at the level $q < 0.1$ in stage III (24–48 h) are shown.

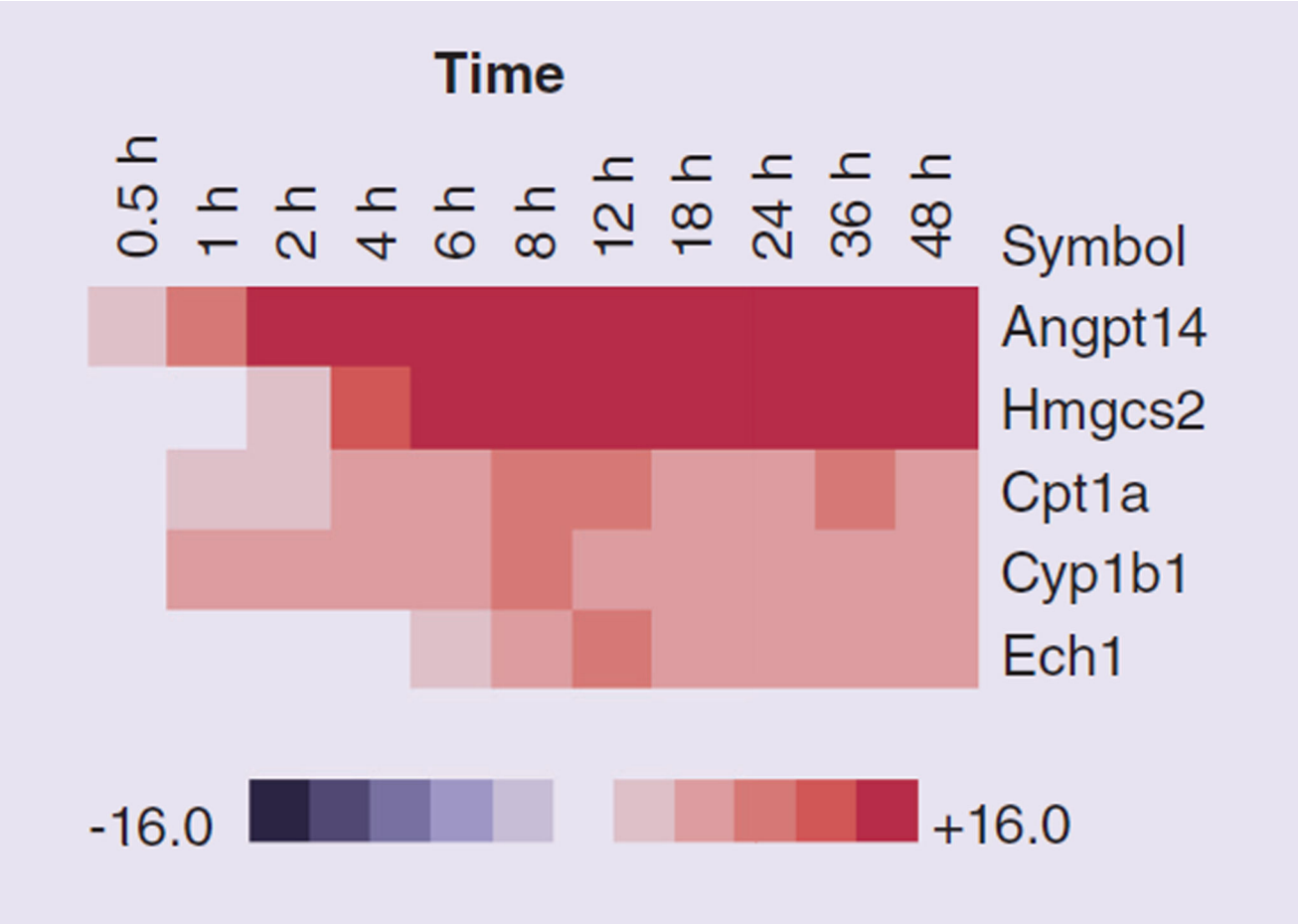

Figure 6. Abundance of transcripts measured by quantitative PCR (relative to a reference gene *GAPDH*) in neonatal rat ventricular myocytes exposed to rosiglitazone or dimethyl sulfoxide control

Red and blue colored boxes depict relative over-and under-expression of the transcripts in rosiglitazone treated cells with respect to control DMSO treated cells at the time point indicated.

Table 1

Biological processes significantly modified in neonatal rat ventricular myocytes exposed to rosiglitazone for 48 h.

GO ID	Biological process	Bonferroni p-value
6955	Immune response	7.06×10^{-19}
6629	Lipid metabolic process	2.74×10^{-17}
33993	Response to lipid	1.06×10^{-9}
9719	Response to endogenous stimulus	3.58×10^{-6}
32879	Regulation of localization	2.1×10^{-5}
72358	Cardiovascular system development	0.000461756
40011	Locomotion	0.003181272

Bonferroni-adjusted p-values are provided.

Table 2

Early stage gene-expression (stage I, 0.5–2 h) responses.

GO ID	Biological process	Bonferroni p-value
72358	Cardiovascular system development	5.72×10^{-7}
48514	Blood vessel morphogenesis	5.80×10^{-7}
71495	Cellular response to endogenous stimulus	0.000102186
70887	Cellular response to chemical stimulus	0.000247052
9719	Response to endogenous stimulus	0.000329665

Biological processes significantly modified following rosiglitazone treatment are presented. Bonferroni-adjusted p-values are provided for nonredundant gene ontology terms.

Table 3

Intermediate stage gene-expression (stage II, 4–18 h) responses.

GO ID	Biological process	Bonferroni p-value
9719	Response to endogenous stimulus	6.06×10^{-10}
9605	Response to external stimulus	2.06×10^{-7}
72358	Cardiovascular system development	7.79×10^{-5}
33993	Response to lipid	0.000226242
70887	Cellular response to chemical stimulus	0.000259545
32879	Regulation of localization	0.000808335

Biological processes significantly modified following rosiglitazone treatment are presented. Bonferroni-adjusted p-values are provided for nonredundant gene ontology terms.

Table 4

Late stage gene-expression (stage III, 24–48 h) responses.

GO ID	Biological process	Bonferroni p-value
6629	Lipid metabolic process	2.30×10^{-15}
9719	Response to endogenous stimulus	9.40×10^{-15}
6955	Immune response	5.02×10^{-14}
70887	Cellular response to chemical stimulus	1.90×10^{-9}
33993	Response to lipid	2.14×10^{-8}
40011	Locomotion	7.25×10^{-8}
32879	Regulation of localization	1.51×10^{-7}
72358	Cardiovascular system development	1.61×10^{-6}
48514	Blood vessel morphogenesis	3.60×10^{-6}
12501	Programmed cell death	0.000580134

Biological processes significantly modified following rosiglitazone treatment are presented. Bonferroni-adjusted p-values are provided for nonredundant gene ontology terms.

Table 5

Late stage gene-expression (stage III, 24–48 h) responses.

GO ID	Cellular component	Bonferroni p-value
44421	Extracellular region part	9.70×10^{-14}
5576	Extracellular region	1.16×10^{-13}
5615	Extracellular space	7.63×10^{-12}
31012	Extracellular matrix	3.46×10^{-9}
9986	Cell surface	8.26×10^{-6}
44459	Plasma membrane part	2.09×10^{-5}
5740	Mitochondrial envelope	7.07×10^{-5}
5739	Mitochondrion	8.01×10^{-5}
5578	Proteinaceous extracellular matrix	1.70×10^{-4}
267	Cell fraction	4.79×10^{-4}
44429	Mitochondrial part	9.15×10^{-4}
31966	Mitochondrial membrane	9.90×10^{-4}

Cellular component terms significantly modified following rosiglitazone treatment are presented. Bonferroni-adjusted p-values are provided.